Modern Environmental Science and Engineering (ISSN 2333-2581)
July 2018, Volume 4, No. 7, pp. 581-589
Doi: 10.15341/mese(2333-2581)/07.04.2018/001
Academic Star Publishing Company, 2018
www.academicstar.us

Effects of One-Point-Scoring Depth on Compressive Strength of Flap-Panel Structure of AB-Flute Corrugated Paperboard

Shigeru Nagasawa, Masanori Yamashita, and Haruya Yokoyama
Nagaoka University of Technology, Japan

Abstract: This paper describes the compressive strength and deformation behavior of folded flap-panel of corrugated paperboard (Cpb). In order to reveal the crushing mechanism of scored Cpb when varying the clearance of bite rolls, a low height flap-panel structure of AB-flute Cpb was experimentally subjected to a quasi-static compressive loading, and the side view of folded zone was analyzed using a video capture. When the panel height of 83mm was compressed up to 12-17% nominal strain, three referenced load points (1st inflection, 2nd peak and 3rd peak) were detected and its corresponded deformation patterns of folded zone were classified in even-slope, wall-digging and flap-digging with respect to the clearance of bite rolls. Also, compared two kinds of fixing condition (flap fixing: IF and wall corner fixing: IF+OF) of folded flap-panel structure, the relationship between the crushing deformation modes and three referenced load points was revealed. The case of IF+OF was apt to be 10~20% stronger than that of IF.

Key words: buckling strength, flap folding, double-wall, bulge, roll gap

1. Introduction

Corrugated paperboard (Cpb) is superior for performing the high strength-to-weight ratio and provides a good shock absorption for transport products. Cpb consists of outer/inner liners and corrugated mediums, and its layered configuration is produced as several combinations: the single face, double face (single wall), double wall (twin cushion) and triple wall [1, 2]. A certain appropriate strength of box structure is required for transporting various packaged products. In order to inspect the performance of compressive strength and design the specification of Cpb box, several compressive resistance tests under static and/or dynamic loading are studied and examined.

Static compressive strength of corrugated box is normally estimated using Kellicut's experimental model [3], which is based on a sum of the ring crush strength with liners and mediums [4] (JIS-P8126, 2005), and its expanded or modified models [5-8]. Since any complicated structures such as double or triple wall were not reported from Kellicut et al., Kawabata proposed advanced-modified Kellicut-Kawabata formula for applying to single and double wall boards [9]. It is necessary to verify the modified factors of compressive box strength with respect to the ring crush strength, when the geometrical profile of corrugated box and the thickness of Cpbs are changed.

Regarding the edgewise compressive strength of Cpb, the end crush test was developed and used [10]. The value of end crush strength is empirically similar to the sum of ring crush strength for all the sheets of Cpb. These estimation models are normally used for designing the strength of corrugated box such as the regular slotted-type container box 0201 (JIS-Z1507: 2013). Therefore, the correlation between geometrical

Corresponding author: Shigeru Nagasawa, Ph.D., Professor, research areas/interests: materials processing, form cutting, sheet bending. E-mail: snaga@mech.nagaokaut.ac.jp.

condition and macroscopic compressive buckling strength is statistically verified for each size of corrugated box. The design formulae are not discussed sufficiently with the elasto-plastic crushing flow of folded zone in the three dimensional distribution. Therefore, a sort of experimental verification is necessary when varying the geometrical conditions of corrugated box.

Regarding theoretical performance of corrugated boxes, there are stress distribution analysis of Cpb using the orthotropic elastic theory [11, 12]. Matsushima et al. analyzed an out-of-plane deflective collapse pattern occurred on a panel of corrugated box, using the elastic model. The in-plane strength of a Cpb was numerically analyzed [13] in terms of edgewise compression of Cpb. Regarding the folding of Cpb, three dimensional bending behavior of score was numerically estimated [14, 15], although its model was fairly simplified. These theoretical analysis works seem to be helpful for knowing an ideal feature of buckling collapse of corrugated box, and predicting the importance of primary design parameters. Seeing these reports, it was confirmed that three dimensional compression of Cpb was theoretically investigated except for discussing the score crushing (lateral-crease folding), and the folding resistance of score in the pre-process was simulated without the compression process of formed box. However, it is empirically obvious that the real compressive strength of corrugated box is affected by the lateral-crease condition (the score gap of creasing bite roller) and the other mechanical conditions which were mentioned above (the sum of ring crush strength, the end crush strength, the box height, width and length). The lateral-crease condition seemed to be embedded as a modification factor in the design formulae, such as Kellicut's model.

In order to reveal the effect of score (lateral-crease) process on the compressive strength of Cpb box, the relationship between the gap (clearance) of creasing rollers and the compressive resistance of folded flap-panel structure should be revealed when choosing the layered configuration of Cpb. Therefore, in this work, the double wall type AB-flute sheet was chosen for the sake of restricting the effect of out-of-plane deflection of panel on the compressive test of flap-panel structure sheet, and the height and width of panel sheets were chosen as relatively small, being 10 times of the thickness of AB-flute sheet. In order to reveal the crushing mechanism of folded zone of laterally-creased AB-flute subjected to a quasi-static compressive loading, a compressive test of folded flap-panel structure was experimentally carried out when varying the clearance of creasing rollers.

2. Experimental Condition for Scoring and Set-up for Compressive Test

2.1 Mechanical Properties of Raw Materials

The layered configuration of AB-flute (double-wall) sheet was shown in Fig. 1. The five layers consisted of (1) the liner of A-flute, (2) the corrugated medium of A-flute, (3) the medium wall between A and B-flute, (4) the corrugated medium of B-flute and (5) the liner of B-flute. The wave length of A and B-flute were $\lambda_A \approx$ 9.0 mm, $\lambda_B \approx$ 6.0 mm, while the height of A and B-flute were t_{MA} = 5.0 mm, t_{MB} = 3.0 mm, respectively. The specimens of AB-flute sheet were prepared as two kinds of configuration using three kinds of raw papers, the mechanical properties of which were shown in Table 1. Namely, Cpb1: Liner 1 (210) – Medium (120): 210-120-120-120-210 and Cpb2: Liner 2 (160) – Medium (120): 160-120-120-120-160 were prepared. Here, the code of five digital values are the layered configuration of (1)-(2)-(3)-(4) described as the basis weight. The height h_O of Cpb1, Cpb2 was 8.0, 7.7 mm, respectively.

Table 2 shows the edgewise crush strength of Cpb1 and Cpb2. According to the rotary creasing condition of AB flute (double wall Cpb) [16, 17], the specimen size of Cpb was prepared as a rectangle which has a width of 230 mm and a length of 320 mm, as shown in Fig. 2. In this work, although the size of width 230 mm and length 320 mm was the same as that of the past condition [17], the longitudinal direction of 320 mm was assigned to MD of Cpb. Namely, the feed (moving) direction of sample sheet matched MD of Cpb.

Three scoring lines, which were at intervals of 80 mm, were processed by the use of rotary scoring apparatus which was illustrated in Fig. 3.

Here, the lower main roll (diameter of D_C = 310 mm) had a carbon-steel wedge bite which had the apex angle of 120 degrees and the tip radius of 0.2 mm, while the

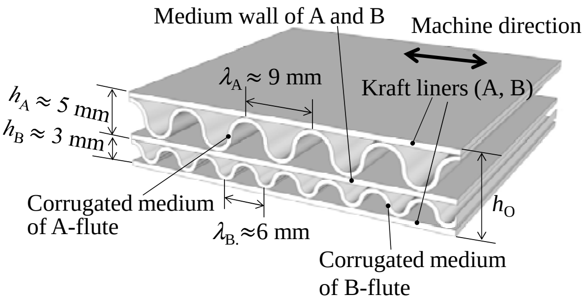

Fig. 1 Layout of double wall corrugated sheet.

Table 1 In-plane mechanical properties of raw paper with corrugated sheet configuration. In-plane tensile test was carried out with feed velocity of 0.33 mm·s^{-1}, based on JIS-P-8113 (2006). Diameter of ring crush test was 48.8 mm, based on JIS P-8126 (2005). MD: machine direction, CD: cross machine direction. Average with ten samples (standard deviation).

	Measured direction &basis weight g·m^{-2}	Thickness t mm	Ultimate strength B MPa	Breaking strain B %	Young's modulus E GPa	Ring crush strength f_{RC} N·mm^{-1}
L1	MD 210	0.24	62 (1.5)	2.1	6.6	2.1 (0.1)
	CD 210		26 (0.3)	5.3	2.5	1.6 (0.06)
L2	MD 160	0.18	39 (0.9)	1.8	5.0	0.9 (0.04)
	CD 160		15 (0.4)	5.0	1.8	0.7 (0.04)
Me	MD 120	0.16	32 (1.9)	1.8	3.3	0.6 (0.05)
	CD 120		14 (0.5)	3.9	1.5	0.4 (0.04)

Table 2 Edgewise crush strength of specimens based on JIS Z-0403-2 (1999), B-method (un-waxed edge).

	Configuration of corrugated sheet (LB: liner boards, MD: mediums)	
Edgewise crush strength f_{EC}/N·mm^{-1}	Cpb-1: LB210-MD120	Cpb-2: LB160-MD120
	7.2 (0.30)	6.0 (0.35)

Average (standard deviation)

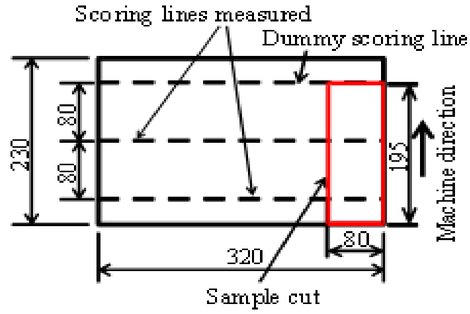

Fig. 2 Dimensions of specimen for scoring. Four samples used for folded flap-panel compressive test were cut off from a scored sheet of 320 mm × 230 mm.

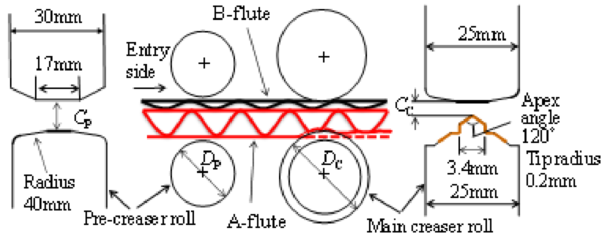

Fig. 3 Schematic diagram of scoring (lateral-creasing) apparatus. A corrugated sheet of 320 mm × 230 mm was scored by using a set of pre-creaser and main-creaser rolls in three lines with distance 80 mm apart. The main creaser roll gap was set as c_C, while the pre-creaser roll gap was set as $c_P > h_O$ (height of sheet).

upper main roll was a carbon-steel plain (flat) roll. The clearance of main rolls was chosen as c_C = 1.0-6.5 mm (as intervals of 0.5 mm), while the rotational speed was 3 rps (circumference velocity of 2.92 m·s^{-1}).

In this case, the A-flute (lower) side was strongly dented. The pre-creaser rolls, which were located in the entry side, had sufficiently a large clearance $c_P > h_O \approx 8$ mm. The pre-creaser rolls were not used for scoring, but for feeding forward. After passing through the scoring apparatus, the scored Cpb of 320 mm × 230 mm was cut off into four specimens with a width of 80 mm by hand working, as shown in Fig. 2. Seeing the main rolls, we need to pay attention that the profile of scoring rolls (for lateral-creasing) is generally different from the prepared profile (one-point type) shown in Fig. 3. This combination of single wedge bite (attacker) and flat anvil (receiver) is called one-point type. Generally, the upper main roll appears to have a dented profile against the lower protruding shape. As other types, three-point type (one bite against two bites with one groove) and five-point type (two bites against three bites) are known [18].

2.2 Experimental Method of Compressive Test

Fig. 4 shows the compressive test apparatus and layout of fixtures with folded flap-panel structure. In Fig. 4 (b), the left side of upper flap (length of 35 mm) and left side of lower flap (length of 80 mm) were fastened by the 1st upper vice and 2nd lower vice, respectively. This fixing condition by two vices was denoted as the inside fixing (IF). Furthermore, the right side of upper folded corner and that of lower folded corner were restricted by the 3rd upper angle beam and 4th lower rectangle beam. The latter fixing condition by the 3rd and 4th JIGs was denoted as the outside fixing (OF). After fixing the worksheet by the use of IF or IF plus OF, the upper cross head was moved downward with the feed velocity of 0.833 mm·s^{-1} until detecting the first inflection point, the second and third peak maximum points denoted as 1, 2 and 3.

As the results, the tracking displacement of cross head was chosen as 10-14 mm (12-17% of height 83 mm). The experiment was carried out under the following conditions: room temperature of 297 K and room humidity of 50% RH. Number of samples was six pieces for each case (when varying the clearance of main rollers under two kinds of fixing conditions).

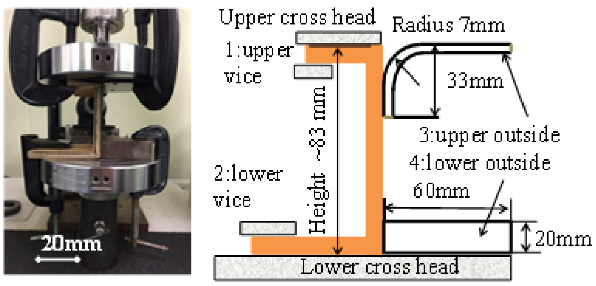

(a) General view (b) Layout of fixtures and specimen

Fig. 4 Compressive test apparatus. A folded AB flute sheet, of which the width was 80 mm, was formed in Fig. 2 and Fig. 3. The panel part of this worksheet was setup in the vertical direction with the height of *L* = 83 mm, and the 1st and 2nd vices clamped the upper/lower flap parts in case of IF condition. Furthermore, in case of full fixing, the OF condition was added to this IF condition.

Fig. 5 illustrated a compressed 0201 type box. Seeing the two parts (red colour) as a folded flap-panel specimen, the fixing condition of middle zone was similar to IF (inside fixing), while that of left side or right side zone was similar to IF plus OF (outside fixing). Namely, the boundary conditions of IF and IF+OF are corresponded to those two positions in the 0201 type box.

3. Results and Discussion

3.1 Set-up Profile of Folded Corner

Fig. 6 shows photographs of folded upper corner of Cpb1 (LB210-MD120) specimen which was initially set-up on the compressive apparatus. Here, the clearance of main rolls were chosen as c_C = 3.5, 4.5, 5.0, 5.5 and 6.5 mm. Seeing those figures, three modes of folding deformation were detected, as shown in Fig. 7.

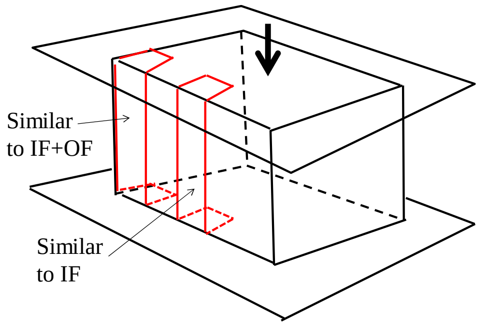

Fig. 5 Physical meaning and roles of IF and OF in the compressed panel. When seeing the middle of wall panel, the outside of wall panel is not restricted, while the left side or right side of wall panel is restricted by the corner of wall panel.

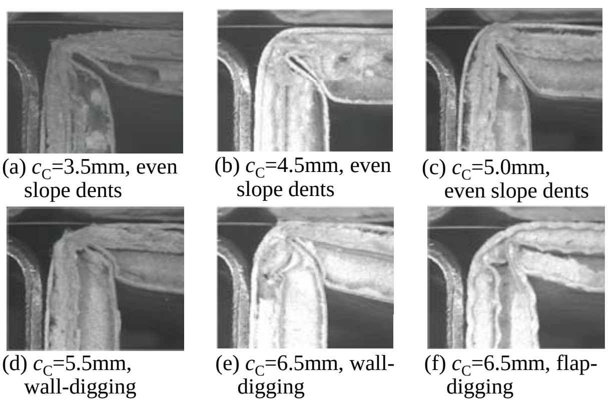

(a) c_C=3.5mm, even slope dents (b) c_C=4.5mm, even slope dents (c) c_C=5.0mm, even slope dents

(d) c_C=5.5mm, wall-digging (e) c_C=6.5mm, wall-digging (f) c_C=6.5mm, flap-digging

Fig. 6 Side views of upper folded corner of Cpb1 (LB210-MD120) at the initial set-up in compressive test apparatus. The fixing condition IF+OF was illustrated.

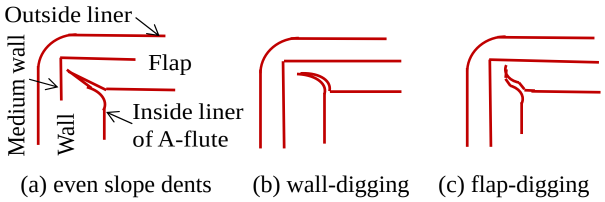

Fig. 7 Classification of folding profile of inside liner of A-flute based on observation of photo-graphs. The mode of even slope dents was detected in case of deep scoring. Two modes of wall-digging and flap-digging occurred when the scoring was insufficient with respect to the medium wall and corrugated medium of B-flute.

When c_C = 1-3.5 mm, the inside liner of A-flute was deeply dented and the dented surface was smoothly folded in even with the vertical and horizontal direction. This mode was named as even slope dents. However, when c_C > 5 mm, due to a shallow scoring, the inside liner of A-flute was apt to be eccentrically folded in either the wall side or flap side. They were named as wall-digging and flap-digging, respectively.

There seems to be an intermediate (transition) state in the region of c_C = 3.5-4.5 mm in the case of Cpb1 specimen. In the case of Cpb2 (LB160-MD120) specimen, the mode of "even slope dents" occurred for c_C < 3 mm, while the modes of "wall-digging" and "flap-digging" were seen for c_C > 3.5 mm. Seeing both Cpb1 and Cpb2 specimens, the scoring gap (clearance) of c_C = 3 mm seems to be a critical condition, for branching the folding mode into two patterns: the even slope dents or the eccentric dents. This appears to be caused by the geometrical height of B-flute.

3.2 Effects of Clearance on Load Response in Com-Pressive Test

Fig. 8 shows examples of compressive line force response with respect to Cpb1, Cpb2 specimens. The first inflection load f_{p1}= 2.5-4 N·mm^{-1} occurred at d_{p1} = 3-5 mm for the both cases: IF and IF+OF. The early stage gradient $k = \partial f / \partial(d/L)$ was estimated as 60-80 N·mm^{-1} for the compressive strain of d/L= 0-0.060 (L = 83 mm). Seeing Table 2, the gradient of line force with flapless panel compression was estimated as k_{EC} = f_{EC}·60/1 = 360$_{(Cpb2)}$, 432$_{(Cpb1)}$ N·mm^{-1}, respectively. Here, the edgewise resistance (end crush test) by the compressive strain of 1/60 was used for calculating the gradient, the stiffness of the flap-panel structure was estimated as 60/360 = 16%, 80/432 = 19% of end crush based gradient. Assuming that k' is the equivalent stiffness of folded and crushed area, the value of k' is estimated using the inverse rule of mixture Eq. (1). Using the estimated values of k and k_{EC}, the value of k' outcomes 144$_{(Cpb2)}$ (= 40% of k_{EC}), 196$_{(Cpb1)}$ (=45% of k_{EC}) N·mm^{-1}, respectively.

$$2/k' = 1/k - 1/k_{EC} \quad (1)$$

After passing through the first inflection point, the compressive resistance tended to be yield up to 10% of d/L in IF, while the compressive resistance of IF+OF had a positive gradient with indentation and was larger than that of IF.

Obviously, the outside restriction by the 3rd and 4th JIGs reinforces the bucking resistance of folded flap-panel structure. Through this compressive test, the inflection and/or peak maximum points 1: (f_{p1}, d_{p1}), 2: (f_{p2}, d_{p2}) and 3: (f_{p3}, d_{p3}) were measured when varying the clearance of main rolls, owing that those three points seem to characterize the compressive strength of

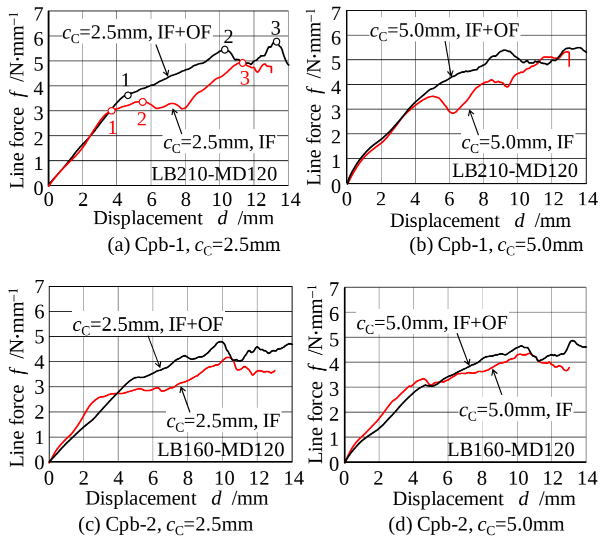

Fig. 8 Relationship between compressive line force and displacement of cross head. The first inflection point was denoted as 1. IF (inside fixing) condition was plotted as red curves, while the both side restriction, IF plus OF (outside fixing) condition, was shown as black curves. The second and third peak maximum points were denoted as 2 and 3, respectively.

folded flap-panel structure. Those three points were illustrated in Fig. 8(a).

Fig. 9 shows the effect of scoring roller gap (clearance of main rolls) on the three referenced loads (the first inflection, the second peak and the third peak line forces) when comparing two kinds of boundary constraints (IF and IF+OF). The three referenced load points were statistically detected when each compressive test was carried out with 66 samples (6 times for 11 kinds of clearance). The state of inflection or peak detection (detected numbers) was varied with the thickness of liner paper. The first inflection load (line force) f_{p1} was appears to be independent from the value of clearance c_C = 1.0-6.5mm. The ratio f_{p1}/f_{EC} was about 0.5 for IF+OF, and 0.42 for IF, respectively.

When using IF, the 2nd peak load (line force) f_{p2} was close to the first inflection f_{p1} especially for c_C = 1-4 mm, while the 3rd peak load f_{p3} was about 30% larger than f_{p1} for c_C = 1-6 mm. To the contrary, f_{p3} was close to f_{p2}, and f_{p1} was about 30% smaller than f_{p2}, when using IF+OF. Synthetically, the ratio f_{p3}/f_{EC} was 0.55-0.8 for Cpb1 and 0.67-0.8 for Cpb2, respectively. The dispersion of peak maximum loads f_{p2} and f_{p3} of Cpb1 was relatively large for $c_C > 3$ mm, while that was small for all the range c_C = 1-6.5 mm in case of Cpb2.

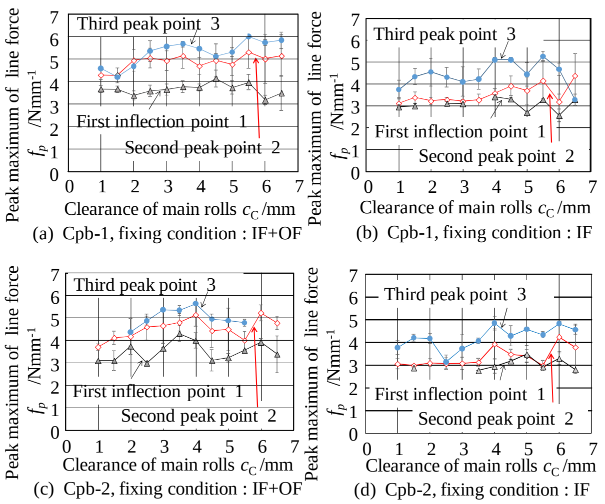

Fig. 9 Relationship between the peak (or inflection) line force of compressive test and clearance of main rolls. Two kinds of specimens (Cpb1 and Cpb2) were arranged with two kinds of boundary constraints (IF, IF+OF).

The increase of dispersion appeared to be caused by a sort of higher order buckling (crushing) of both the outside and inside liner.

3.3 Crushed Profile of Folded Corner in Compressive Test

Fig. 10 shows the sectional views of folded upper corner of Cpb1 subjected to a compressive load, when the clearance of main rolls has been chosen as c_C= 2.5 mm. Here, the fixing condition of specimen was chosen as IF+OF for Fig. 10 (a), (b) and (c), while that was chosen as IF for Fig. 10 (d), (e) and (f). In these pictures, a yellow or red circle corresponded to the same particle detected in each specimen. Similarly, Fig. 11 shows that of Cpb2 when c_C =2.5 mm.

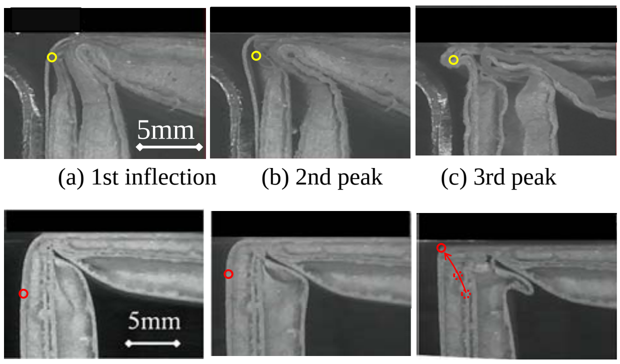

(a) 1st inflection (b) 2nd peak (c) 3rd peak
(d) 1st inflection (e) 2nd peak (f) 3rd peak

Fig. 10 Photographs of side views of folded upper corner of Cpb1 sheets (LB210-MD120), which were scored with c_C = 2.5 mm. The fixing condition of (a)-(c) was chosen as IF+OF, while that of (d)-(f) was chosen as IF.

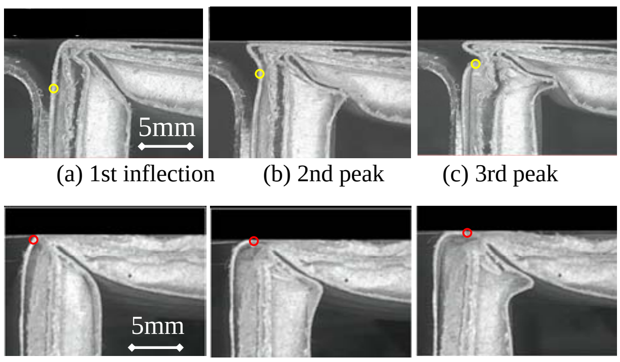

(a) 1st inflection (b) 2nd peak (c) 3rd peak
(d) 1st inflection (e) 2nd peak (f) 3rd peak

Fig. 11 Photographs of side views of folded upper corner of Cpb2 sheets (LB160-MD120), which were scored with c_C = 2.5 mm. The fixing condition of (a)-(c) was chosen as IF+OF, while that of (d)-(f) was chosen as IF.

Seeing the deformation modes of liners and mediums, several features were detected as follow: (i) The inside liner of A-flute is dented and folded sufficiently at the first inflection point. Its folded surfaces contacted with each other, as shown in Fig. 10 (a), (d) and Fig. 11 (a), (d). (ii) Seeing the particle motion of yellow circles under IF+OF condition, their positions were almost not changed during the cross head indentation. On the contrary, seeing the red circle under IF condition in Fig. 10(d)-(f), the red circle position moved about 3 mm on the left side (toward outside). This lateral expansion contributes to reduce the contact pressure resistance between the flap and wall of inside liner of A-flute. As the result, the second peak f_{p2} remarkably decreased in the case of IF condition. In the case of Fig. 11(d)-(f), the red circle appeared to be paused at the same position and the left wall (liner) moved about 3mm on the left side. (iii) Comparing the thick liner of LB210 (Cpb1) with the thin liners of LB160 (Cpb2) in Fig. 8, the occurrence timing of second and third peak points tended to be postponed in IF+OF condition. As the result, the medium wall of Cpb1 was supposed to be not crushed yet at the first inflection, while that of Cpb2 was obviously crushed at the first inflection point. At the second peak position, the outside liner and inside liner were extremely crushed (upset) in the Cpb2, while that were just before upset crushing in the Cpb1. (iv) Before reaching the 1st inflection, the B-flute composed of the outer liner and middle wall appears to resist against the compressive load. When the inside liner of A-flute buckled and make two bulges in contact, this structure seems to make the secondary stiffness shown as the inflection slope. (v) Seeing the 2nd and 3rd peak points in the case of IF+OF, the outside liner was crushed against the upper cross head. The 2nd peak is related to the crushing of outside liner of B-flute, while the 3rd peak seems to consist of the crushing of B-flute liner and the higher order buckling of inside liner of A-flute, as shown in Fig. 10(c) and Fig. 11(c).

Through the consistent discussion with the crushing profile of folded corner and its related load characteristics, it was found that the folded corner of specimen under IF was crushed and expanded to the outside, while that part under IF+OF condition was crushed without moving outward. As the result, the former was composed of the 1st inflection and the stationery-outward flow of crushed outside liner and medium wall, and the latter was determined by the high order local buckling of outside liner and medium wall. Those two fixing conditions seem to occur at the compressive test of a 0201 type box. On the panel of wall, the middle position in the 0201 type appeared to behave as the IF condition, while the corner position in the 0201 type box appeared to be the IF+OF condition, due to the folded corner structure. Therefore, on the panel of wall, there are two modes: the IF condition and IF+OF condition.

4. Conclusions

Seeing the in-process deformation of folded flap-wall corner and the referenced load points, the following results were revealed.

(1) At the initial set-up of compressive test, the crushed profile of folded corner was classified in three modes: (a) the even slope dent which occurred in case of deep scoring $c_C < 3$ mm, (b) the wall-digging and (c) the flap-digging. The latter deformation (b), (c) were detected in case of shallow scoring $c_C > 3$ mm. This branching occurrence of (b), (c) appeared to be statistically random but this branching affected the dispersion of 2nd and 3rd peak line forces which were formed from a high order crushing (buckling). Here, the critical value of $c_C = 3$ mm was related to the height of outside layer (B-flute).

(2) The ratio of first inflection line force by the end crush strength f_{p1}/f_{EC} was about 0.5 for IF+OF, and it was 0.42 for IF, respectively. Its average value was independent from the variance of the main roll gap for c_C = 1.0-6.5 mm, while the dispersion of its value varied with c_C, especially for $c_C > 3$ mm.

(3) The ratio of third peak line force by the end crush strength f_{p3}/f_{EC} was about 0.6 (IF), 0.8 (IF+OF) for Cpb1 and 0.7 (IF), 0.8 (IF+OF) for Cpb2, respectively. The case of IF+OF was 10~20% stronger than that of IF.

(4) The initial gradient of load increasing by the indentation (in-plane stiffness along the wall panel) k was estimated as k/k_{EC} = 16% for Cpb2, 19% for Cpb1, respectively. Here, k_{EC} was the ratio of f_{EC} by the compressed strain (1/60). Using the inverse rule of mixture, the equivalent spring of folded and crushed area k'/k_{EC} was estimated as 40% for Cpb2 and 45% for Cpb1, respectively.

(5) In the condition of flap inside fixing (IF), the outside layer (B-flute) was continuously crushed and the folded corner moved to the outside. Also, the inside liner of A-flute moved to the outside. On the contrary, in the case of flap inside and wall outside fixing (IF+OF), the crushing position of work material did not almost flow out, due to existing of the outside fixing blocks.

Acknowledgements

This work was supported by a fund for developing a core of excellence as innovative and branding project, from the GIGAKU Innovation Promotion Center, NUT, 2016-2017. The authors wish to thank Mr. Atsushi Watanabe, who is a master's graduate of NUT, for his support on investigating the compressive test of rectangle panels without flaps.

References

[1] R. Steadman, Characterization of corrugated board, in: *Handbook of Physical Testing of Paper* (2nd ed.), Marcel Dekker, 2002, pp. 571-574.

[2] A. Dekker, Corrugated fiberboard packaging, in: *Handbook of Paper and Paperboard Pacakaging Technology* (2nd ed.), Wiley-Blackwell, 2013, pp. 313-321.

[3] K. O. Kellicutt and E. F. Landt, Basic design data for the use of fiberboard in shipping containers, *Fiber Containers* 36 (1951) (12) 62-80.

[4] C. Fellers and B. C. Donner, Ring crush test, in: *Handbook of Physical Testing of Paper* (2nd ed.), 1, Marcel Dekker, 2002, pp. 510-513.

[5] R. C. Mackee and J. W. Gander, Top load compression, *TAPPI (Technical Association of the Pulp and Paper Industry)* 40 (1957) (1) 57-64.

[6] R. C. Mackee, J. W. Grander and J. R. Wachuta, Compression strength formula for corrugated boxes, *Paperboard Package* 48 (1963) (8) 149-159.

[7] M. Wolf, *How Box Length, Width Affects Compression Strength*, Package Engineering, October, 1971, pp. 68-70.

[8] R. Steadman, Box compression resistance, *Handbook of Physical Testing of Paper* (2nd ed.), 1, Marcel Dekker, 2002, pp. 582-592.

[9] Y. Kawabata, Compression strength of corrugated box (1): Establishing of new constants for Kellicut's equation, *Journal of Packaging Sci. and Technol. Japan* 6 (1997) (1) 19-28.

[10] W. O. Kroeschell, The edge crush test of corrugated board: Development of TAPPI test methods T811 & T823, *TAPPI (Technical Association of the Pulp and Paper Industry)* 67 (1984) (10) 56-58.

[11] S. Matushima and S. Matsushima, Elastic deformation analysis of corrugated fiberboard box under uniform compressive displacement on upper and lower edges: Elastic analysis for square tube, *Transactions of Japan Soc. Mech. Eng. Series A* 72 (2006) (716) 535-542.

[12] S. Matushima and S. Matsushima, Elastic bending stress analysis of fracture line generation for case (square tube) of corrugated fiberboard box shape under uniform compression loading: On panel height/width = 0.8−2, *Transactions of Japan Soc. Mech. Eng. Series A* 73 (2007) (726) 181-188.

[13] E. Mikami, T. Ibaraki, T. Kobayashi and I. Kodaka, Finite element analysis for edgewise compression of corrugated fiberboard, *Journal of Packaging Sci. and Technol. Japan* 3 (2004) (4) 243-252.

[14] H. Ishibuchi, S. Nagasawa, A. Yoshizawa and Y. Yoshitani, Three-dimensional bending stress analysis for corrugated fiberboard sheet, *Transactions of Japan Soc. Mech. Eng. Series A* 60 (1994) (580) 2774-2781.

[15] H. Ishibuchi, S. Nagasawa, A. Yoshizawa and Y. Yoshitani, Study of bending work of corrugated fiberboard sheet, *Journal Japan Soc. Technol. Plasticity* 36 (1995) (416) 917-925.

[16] S. Nagasawa and Y. Komiyama, Effect of Scoring condition on creasing characteristics of double-wall corrugated board, *Journal of Advanced Mechanical Design, Systems, and Manufacturing* 6 (2012) (7) 1263-1272.

[17] S. Nagasawa, K. Ishibashi and Y. Fukuzawa, Effect of pre-creasing roller shape on creasing characteristics of double-wall corrugated board, in: *Proceeding Book of*

International Conference on Materials Processing Technology, Bangkok, 2013, pp. 171-176.

[18] S. Igarashi, *Packaging Technology of Corrugated Board, Practical Part*, Nippo Publishing. 2012, pp. 245-256.